Journal of Molecular Catalysis A: Chemical 395 (2014) 315–321

Contents lists available at ScienceDirect

Journal of Molecular Catalysis A: Chemical

journal homepage: www.elsevier.com/locate/molcata

Influence of heat treatment on catalytic performance of Co–N–C/SiO_2 for selective oxidation of ethylbenzene

Zhi-Gang Liu*, Lin-Tao Ji, Jia Liu, Ling-Ling Fu, Su-Fang Zhao

School of Chemistry and Chemical Engineering, Hunan University, Changsha 410082, China

ARTICLE INFO

Article history:
Received 21 June 2014
Received in revised form 25 July 2014
Accepted 29 July 2014
Available online 7 August 2014

Keywords:
Co–N–C/SiO_2
Co–N_4–C
Supported metalloporphyrin
Heat treatment
Ethylbenzene oxidation

ABSTRACT

The effect of heat treatment on the Co–N–C/SiO_2 catalysts prepared through supported metalloporphyrin has been investigated for selective oxidation of ethylbenzene. And techniques such as BET, XRD, FT-IR, UV–vis, TEM, TG–DTA and XPS are used to explore the relationship between heat temperature and the catalytic performance of the catalysts. The results show that Co–N–C/SiO_2 catalyst heated at 500 °C exhibits much higher activity for ethylbenzene oxidation compared with its counterparts such as Co–N–C/SiO_2 catalysts heated at 300 °C, 400 °C, 600 °C and 700 °C, respectively. This may be attributed to the formation of much more Co–N_4–C active sites on the surface of Co–N–C/SiO_2 catalyst heated at 500 °C.

1. Introduction

Selective oxidation of alkane to aldehyde or ketone has attracted a lot of attention in the past decades, as these products are important intermediates for the synthesis of fine chemicals. Moreover, it presents the possibility of using renewable biomass-derived feedstock [1–3]. Typically, from the viewpoint of sustainable and green chemistry, molecular oxygen is recommended to use as clean oxidants [2]. However, this requires preparation of highly active, selective, and recyclable O_2-activating heterogeneous catalysts [3].

Fe and Co porphyrin or phthalocyanine have emerged and been reported as promising candidates due to their economical cost and catalytic performance as well as that of precious metals [4–6]. For example, in our group, Shen et al. [7] have reported that immobilized Mn porphyrin on hybrid nanocomposite microspheres and the catalytic performance of the as-prepared catalysts was significantly enhanced, and the conversion of ethylbenzene was up to 22.9%. The catalyst also possessed high stability, and could be reused six times without remarkable loss of the catalytic activity. These catalysts displayed remarkable activity and selectivity to ethylbenzene oxidation, compared to the unsupported counterpart. However, the supported metalloporphyrin suffered from disability and comparable low conversion of ethylbenzene due to the drawbacks such as easy deactivation.

Since 1960s, heat treatment of transition metal macrocycles has been reported to be an effective way to improve the catalytic performance of the catalysts. For example, Maldonado et al. [8,9] reported that the heat treatment of M-macrocycles in an inert atmosphere can significantly improve activity as well as stability. Jiang and Chu [10] prepared heat-treated CoTPP/FeTPP, which showed better catalytic activity than the corresponding catalysts containing single metals. Gouerec et al. [11] found that CoTAA/C heat-treated at 600 °C showed the best performance in terms of activity and durability. Moreover, it has been pointed out that even when metallic centers are not chemically bound to the macrocycle, highly active sites can be obtained after heat treatment [12].

In this study, SiO_2 is used as the support to immobilize metalloporphyrin, because it allows for ease of modification and immobilization of the metal precursor onto its surface. And Co–N–C/SiO_2 catalysts are prepared via heat treatment of supported metalloporphyrin. The effect of heat treatment on the properties of Co–N–C/SiO_2 and their catalytic performance for ethylbenzene oxidation are investigated. Catalysts were characterized by N_2 adsorption and desorption (BET), Fourier Transform infrared spectrometer (FT-IR), UV–visible spectroscopy (UV–vis), transmission electron microscopy (TEM), thermogravimetry–differential thermal analysis (TG–DTA) and X-ray photoelectron spectroscopy (XPS).

* Corresponding author. Tel.: +86 731 8882 3327.
E-mail addresses: liuzhigang@hnu.edu.cn, cerialiu@gmail.com (Z.-G. Liu).

http://dx.doi.org/10.1016/j.molcata.2014.07.032
1381-1169/

2. Experimental

2.1. Synthesis of cobalt (II)5-(4-carboxyphenyl)-10,15,20-triphenyl porphyrin (CoTPP)

The compound was synthesized according to the literature [7]. Typically, 4.69 g of distilled pyrrole was added dropwise into a three-neck flask containing a mixture of 250 mL propanoic acid, 5.56 g benzaldehyde and 2.62 g 4-carboxy benzaldehyde, and then heated to reflux for 30 min. And the resultant product was cooled overnight, then filtered and purified. 5-(4-Carboxyphenyl)-10,15,20-triphenyl porphyrin was obtained. 1.0 g of the as-synthesized sample was dissolved in 100 mL N,N-dimethylformamide (DMF). After 2.5 g of $CoCl_2{\cdot}6H_2O$ was loaded, mixture was heated to reflux under stirring until porphyrin was exhausted. Cooling overnight, the obtained mixture was filtered and washed repeatedly with hot water, and the product, denoted as CoTPP, was achieved.

2.2. Synthesis of NH_2–SiO_2

The amine-functionalized SiO_2 were prepared as described in literature [13]. In a typical procedure, SiO_2 (1.0 g) and 15 mL 3-aminopropyltrimethoxysilane (APTES) were added into 30 mL methylbenzene under vigorous stirring at 60 °C for 24 h. The white solid was centrifuged and washed with methylbenzene and ethanol in order to remove solvent and residual APTES. And then dried overnight at 80 °C, the obtained product was denoted as SN.

2.3. Synthesis of Co–N–C/SiO_2 catalysts

Co–N–C/SiO_2 catalyst was prepared by heat treatment of supported metalloporphyrin. Supported metalloporphyrin was prepared as following. 0.01 g CoTPP and 0.10 g SN were dispersed in 20 mL of dichloromethane at 40 °C for 24 h. After centrifugation and drying at 80 °C overnight, supported metalloporphyrin was achieved, denoted as CoTPP/SiO_2, and heated in nitrogen atmosphere in the range from 300 °C to 800 °C for 1 h, respectively. And the products are denoted as Co–N–C-*X*/SiO_2 (where *X* means heat temperatures). For example, the sample heated at 500 °C is denoted as Co–N–C-500/SiO_2.

2.4. Characterization of catalysts

Surface area was measured by nitrogen adsorption/desorption at −196 °C on an Autosorb-6b apparatus from Quanta Chrome Instruments. The samples were degassed at 160 °C for 2 h prior to the adsorption experiments. FT-IR spectra were carried out on a Vertex 70 (Bruker) Fourier transform infrared spectrometer. UV–vis diffuse reflectance spectra of solid samples were collected on the Shimadzu 2450 spectrophotometer. The morphology of samples was measured by a transmission electron microscopy (TEM, JEM-2100F) with an electron microscope operating at an 80 kV voltage. TG–DTA was carried out on a Shimadzu TG/DTA 60 thermal analyzer. The sample was placed in platinum crucible (0.1 cm^3) and measured under N_2 atmosphere with flowing rate of 30 mL/min. The heat rate was fixed at 10 °C/min when heating temperature was raised from 50 to 800 °C. X-ray photoelectron spectroscopy (XPS) measurements were performed with a RBD upgraded PHI-5000C ESCA system (Perkin Elmer) with Mg Kα radiation ($h\nu$ = 1253.6 eV) or Al Kα radiation ($h\nu$ = 1486.6 eV). The obtained binding energies were calibrated using the C_{1s} peak at 284.6 eV as reference.

Table 1
The surface areas and pore volume of Co–N–C/SiO_2 catalysts.

Sample	BET surface area (m^2/g)	Pore volume (ml/g)
SN	30.8	0.092
Co–N–C-300/SiO_2	11.3	0.013
Co–N–C-400/SiO_2	14.9	0.019
Co–N–C-500/SiO_2	24.6	0.031
Co–N–C-600/SiO_2	19.5	0.023
Co–N–C-700/SiO_2	17.6	0.016

2.5. Measurement of catalytic activity

The selective oxidation of ethylbenzene with molecular oxygen was conducted in a 50 mL autoclave. 10 mL of ethylbenzene and 30 mg catalyst were loaded in the reactor and then sealed and raised pressure to 8.0 atm with O_2. Following that, temperature was elevated to 120 °C and kept for 5 h. The products are analyzed by gas chromatography (ShimadzuGC-2014 equipped with a capillary column (RTX-5, 30 m, ϕ0.25 mm) with internal standard method using bromobenzene and 1,4-dichlorobenzene as reference. The recovered catalyst was obtained by centrifugation, then washed with ethanol and dried at 80 °C for 12 h.

3. Results and discussion

3.1. Catalyst characterization

3.1.1. BET

The BET surface areas of Co–N–C/SiO_2 together with SN are listed in Table 1. The surface area of SN is 30.8 m^2/g, much larger than those of Co–N–C/SiO_2. Evidently, metalloporphyrin and/or their heat treatment residual have leaded to the elimination of surface area by blocking or covering the pores in SN. Moreover, when heat temperature is in the range from 300 °C to 700 °C, the surface area of Co–N–C/SiO_2 initially keeps increasing from 11.3 m^2/g of Co–N–C-300/SiO_2, and after Co–N–C-500/SiO_2 reaches 24.6 m^2/g, the surface area of Co–N–C-700/SiO_2 is lowered to 17.6 m^2/g in the end. Apparently, in this process, heat treatment plays an important role in determining the surface area and pore volume of Co–N–C/SiO_2. This may attributed to the formation of new pores in the surface of Co–N–C/SiO_2 at low temperature such as 300 °C or 400 °C and the pores will be blocked due to the collapse of the pores after high temperature such as 600 °C or 700 °C. Moreover, the carbonized residual, which may plug into the small pores, has a negative effect on the BET surface area. The reduction of small pores results in the decrease of surface areas [14].

3.1.2. FT-IR

FT-IR spectra of SN, SiO_2 and Co–N–C/SiO_2 are shown in Fig. 1, the peaks around 3400 cm^{-1} and 1630 cm^{-1} are attributed to silanol group and adsorbed water [15]. C–H bending vibration in unhydrolyzed-OEt groups are observed between 1350 and 1500 cm^{-1} [16]. Bands located at 1101, 945, 802 and 476 cm^{-1} are associated with the longitudinal-optical (LO) mode and transverse-optical (TO) mode of Si–O–Si asymmetric bond stretching vibration, Si–OH stretching vibration, and network Si–O–Si symmetric bond stretching vibration, respectively [16].

As shown in Fig. 1, the peak at 945 cm^{-1} is gradually reduced with the elevation of heat temperature. This is assigned to the elimination of Si–OH. As a result, the reduction of Si–OH group will cause the collapse of pores in SN. This is also correlated with the trend of surface area of Co–N–C/SiO_2. In addition, except the characteristic peaks of SiO_2, there is no more peak to be found. This may be due to the content of metalloporphyrin residual lower than the sensitivity of the detector in FT-IR spectrum instrument.

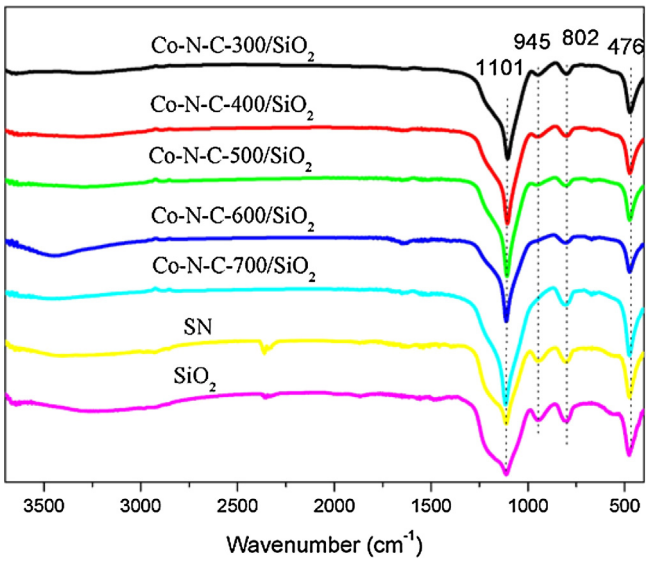

Fig. 1. FT-IR spectra of the catalysts.

3.1.3. UV–vis

The solid UV–vis spectra of CoTPP, CoTPP/SiO_2 and Co–N–C/SiO_2 are shown in Fig. 2. The Soret band at 428 nm, i.e. the characteristic peak of porphyrin rings, can be found in UV–vis spectra of CoTPP and CoTPP/SiO_2 [17]. This means metalloporphyrin has been immobilized on SN nanospheres and porphyrin rings are still in good shape in CoTPP/SiO_2. However, the intensity of Soret band of CoTPP/SiO_2, compared with that of CoTPP, is lowered due to the effect of support and low metalloporphyrin content. Moreover, as for the supported metalloporphyrin, a slight blueshift in Soret bands is observed in comparison with homogeneous metalloporphyrin. This can be explained by the interaction between metalloporphyrin and SN nanospheres [7]. When CoTPP is functionalized onto SN nanosphere surface, the interaction between CoTPP and the functional groups on the surface of SN nanospheres may change the symmetry of porphyrin. As a result, the adsorption bands shift toward higher energy. With respect to Co–N–C/SiO_2, the characteristic peaks of metalloporphyrin are not detected, due to the destruction of porphyrin rings after heat treatment at temperatures as high as 300 °C or even higher temperatures. This means that porphyrin rings are destroyed in inert atmosphere at high temperatures [18–22].

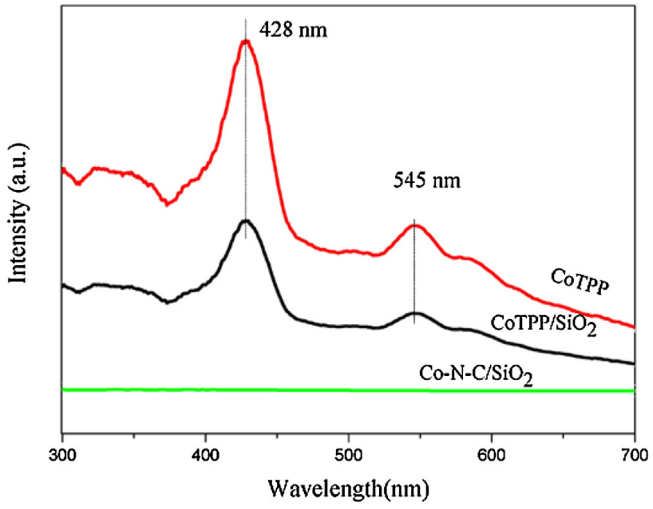

Fig. 2. UV–vis spectra of CoTPP, CoTPP/SiO_2 and Co–N–C/SiO_2.

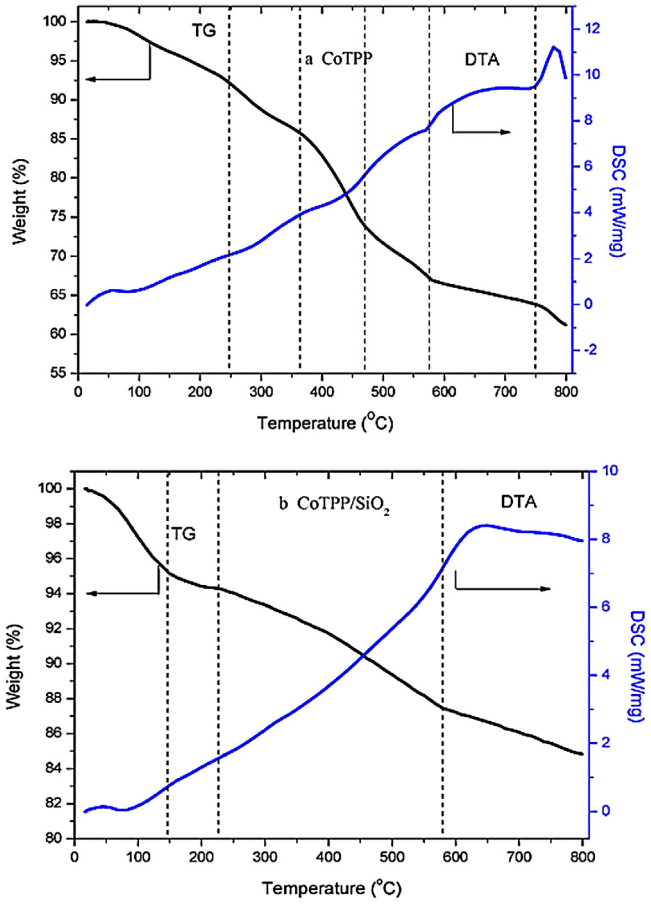

Fig. 3. TG–DTA patterns of CoTPP and CoTPP/SiO_2 in N_2 atmosphere.

3.1.4. TG–DTA

Thermal stability of CoTPP and CoTPP/SiO_2 has been determined by TG–DTA. As depicted in Fig. 3, the curve describes that CoTPP and CoTPP/SiO_2 are treated in N_2 atmosphere at temperatures in the range from 30 °C to 800 °C with a heat rate of 20 °C/min.

In Fig. 3a, the TG–DTA curves describe the heat-treatment procedure of CoTPP in N_2 atmosphere. Despite decades of work in this field, there is still not fully understood about this process. But general steps during the heat treatment of CoTPP are described as following [23,24]. Initially, weight loss at 220–350 °C is due to dehydration. When temperature is raised to about 350–470 °C, carbon oxides are released due to decarboxylation and the polymerization of metalloporphyrin is completed. Then the decomposition of CoTPP-like polymer is responsible for the weight loss at 470–580 °C. During this step, pyrolysis of the polymer is going on to produce fragments containing Co bound to C and N on the catalyst surface. Some of the fragments may be involved in the Co–N_4 moiety. When temperature is higher than 580 °C, Co can still be detected, and some of the fragments may be decomposed to Co–N_2 moiety. As for the weight loss at temperature higher than 750 °C, breaking Co–N and Co–O bonds is responsible for.

However, as shown in Fig. 3b, CoTPP/SiO_2 shows somewhat different decomposition behavior due to covalent interactions between CoTPP and SN. The initial weight loss below 150 °C is due to desorption of water. As the temperature is raised to 230 °C, the weight loss of the sample becomes rapid. At about 580 °C, this process is alleviated as described in the TG–DTA curves. Here, the support, i.e. SiO_2, is the main part in CoTPP/SiO_2 (the content of CoTPP is 0.3 wt%). Therefore, dehydration of residual Si–OH in CoTPP/SiO_2 is responsible for the weight loss during

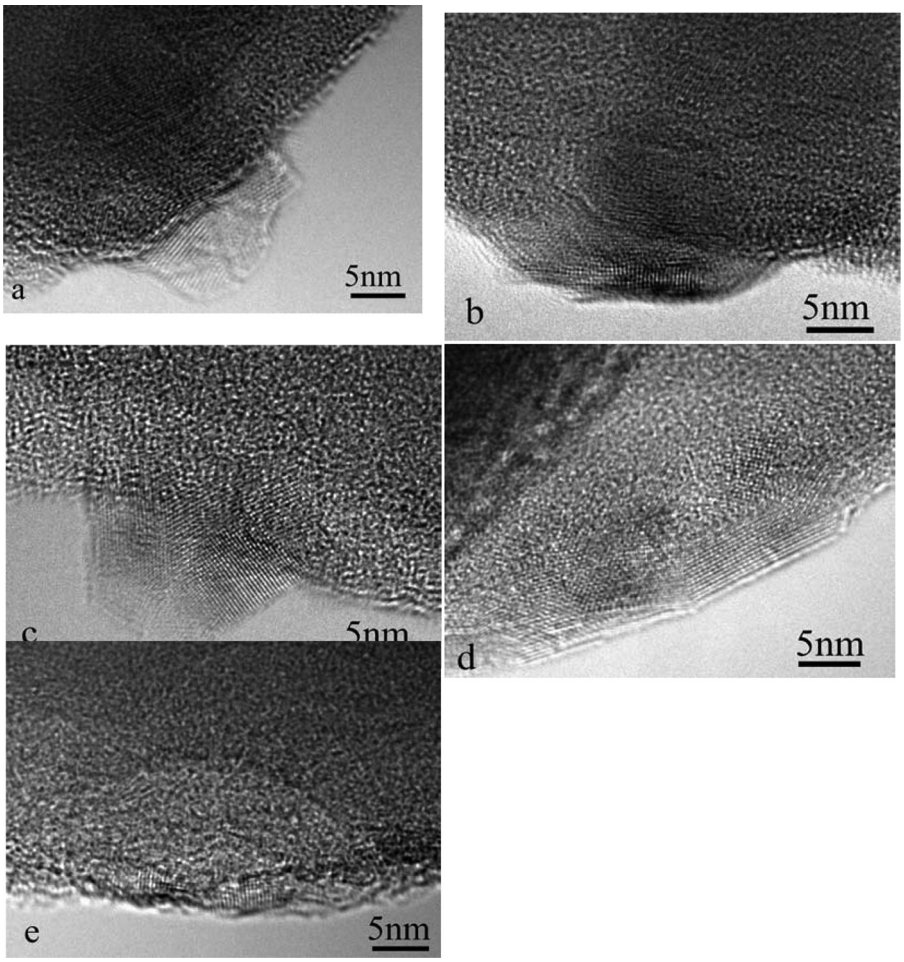

Fig. 4. TEM images of Co–N–C/SiO_2 catalyst. (a) Co–N–C-300/SiO_2, (b) Co–N–C-400/SiO_2, (c) Co–N–C-500/SiO_2, (d) Co–N–C-600/SiO_2, (e) Co–N–C-700/SiO_2.

the thermal treatment. However, it is also well known that the heat treatment of the support in inert gas can lead to a loss of oxygen surface groups through their decomposition, resulting in better resistance of the support against corrosion. Apparently, the heat treatment of CoTPP/SiO_2 may facilitate the stability of Co–N–C/SiO_2.

3.1.5. TEM

TEM micrographs can discern the morphology of supported catalysts. In this study, the active sites are immobilized on uniform silica spheres with particle sizes of about 300 nm prepared by stokes method. Herein, as shown in Fig. 4, the well dispersed cobalt complex with particle sizes of about 5 nm, such as CoO_x and CoN_x, is comparably small in comparison with the sizes of silica spheres. Especially, the particle sizes of these cobalt complexes are almost similar even when they have been heated at temperatures in the range from 300 to 800 °C. Obviously, the formation of Co–N–C on SiO_2 surface is helpful to hinder the particle growth at high heating temperature. This may be attributed to the interaction between active centers and supports. Furthermore, graphite originated from the organic precursors may also protect cobalt complexes from growing up at high heat temperatures.

In Fig. 4a and c, as for Co–N–C-300/SiO_2, the island-like cobalt complexes are presented on silica surface, which are proposed to be the active sites. Generally speaking, the sites exposed at the edges of the plate are the actual active centers because only these active sites are accessible in many reactions [25,26]. For all Co–N–C/SiO_2, the island-like structures are found with almost similar particle sizes, which suggests that the particle sizes may not the determining factor to the catalytic activity of Co–N–C/SiO_2.

3.1.6. XPS

As shown in Table 2, XPS analysis of Co_{2p}, N_{1s}, O_{1s} and C_{1s} of Co–N–C/SiO_2 catalysts was carried out to identify the chemical states of surface elements, which can correlate the activity of the catalyst with their chemical composition. The heat treatment is required for the formation of the active sites for ethylbenzene oxidation [8,9]. However, heat treatment of the Co–N–C/SiO_2 at high temperature will lead to modify the surface composition.

Among the surface composition in Co–N–C/SiO_2, the content of C is the largest part. Moreover, with the heat temperature increases, the contents of C in Co–N–C-300/SiO_2, Co–N–C-500/SiO_2 and Co–N–C-700/SiO_2 reach 54.44%, 57.15% and 61.33%, respectively. Apparently, heat is beneficial to produce more carbon on the surface. Interestingly, the content of Co has a similar trend. Namely, with the heat temperature increases, the contents of Co in Co–N–C-300/SiO_2, Co–N–C-500/SiO_2 and Co–N–C-700/SiO_2 reach 0.31%, 0.36% and 0.42%, respectively. This may be attributed to the shift of Co to the surface on Co–N–C/SiO_2, when suffered heat treatment.

However, oxygen-containing functional groups derived from the catalyst are removed after further heat treatment in N_2 atmosphere. Herein, the contents of O in Co–N–C-300/SiO_2, Co–N–C-500/SiO_2 and Co–N–C-700/SiO_2 decrease from 31.08% to 28.84% and then to 25.72% when heat temperatures are elevated. At the same time, the contents of Si are lowered. This should be the

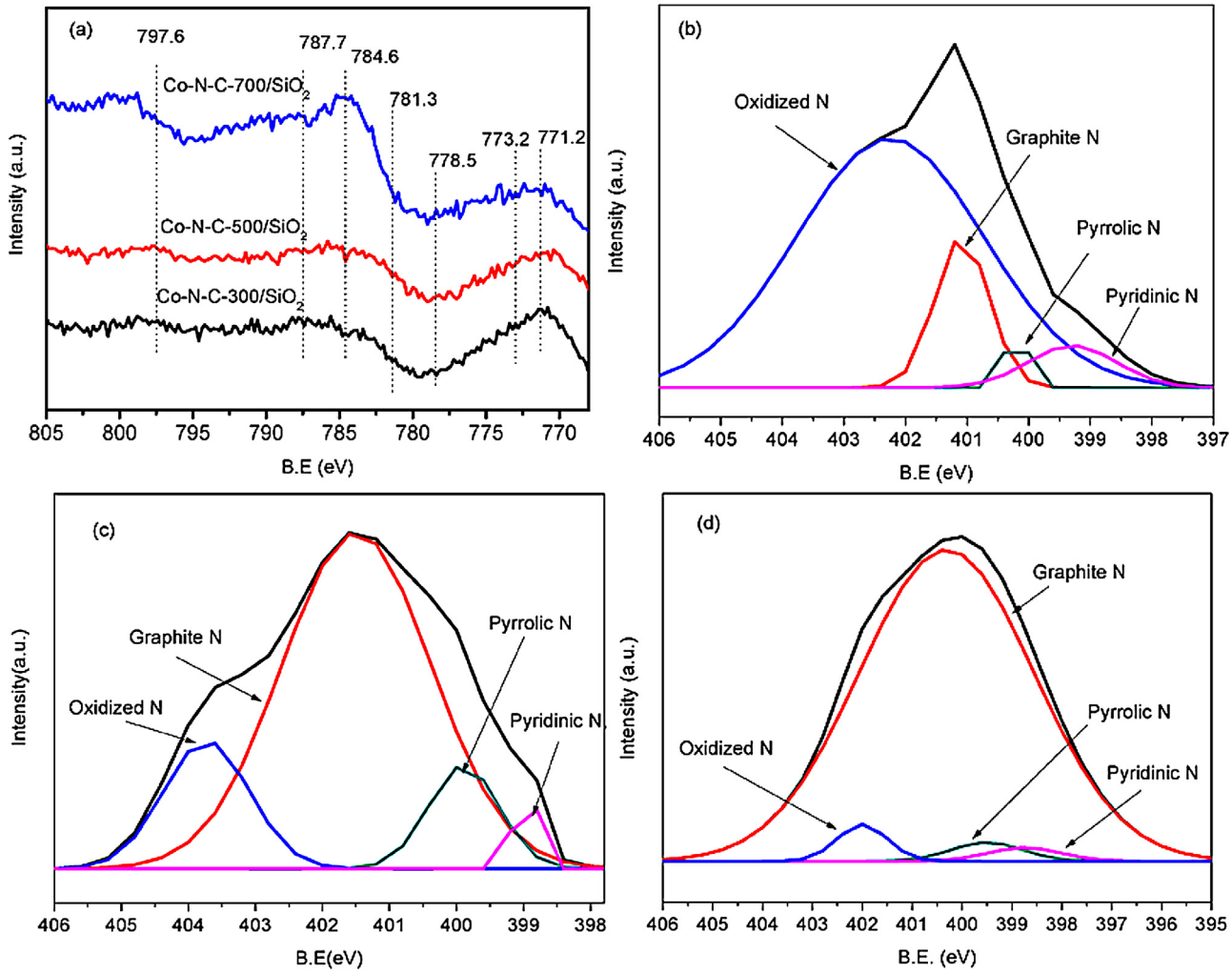

Fig. 5. (a) Co_{2p} XPS spectra of Co–N–C-300/SiO_2, Co–N–C-500/SiO_2 and Co–N–C-700/SiO_2, (b) decomposed N_{1s} XPS spectra of Co–N–C-300/SiO_2, (c) decomposed N_{1s} XPS spectra of Co–N–C-500/SiO_2, (d) decomposed N_{1s} XPS spectra of Co–N–C-700/SiO_2.

fact that more and more carbon is formed to cover Si on the surface with the increase of heat temperatures.

It is worth to note that the contents of N in Co–N–C-300/SiO_2, Co–N–C-500/SiO_2 and Co–N–C-700/SiO_2 do not meet a linear trend. That is, the content of N in Co–N–C-500/SiO_2 is 1.12%, smaller than 1.37% in Co–N–C-300/SiO_2 and 2.15% in Co–N–C-700/SiO_2.

As shown in Fig. 5a, the Co_{2p} core level peak produced $Co_{2p3/2}$ and $Co_{2p1/2}$ peak at 771.2, 778.5, 781.3 and 797.6 eV, respectively, which could be ascribed to the lattice cobaltous oxide [27]. This shown that the surface of catalysts contained a mixture of Co^{3+} and Co^{2+}. In addition, the peak at 781.3 eV is due to the cobalt associated with N in Co–N_x structures. Furthermore, N has been considered to be essential for Co–N–C/SiO_2 to achieve high catalytic performance [28].

The decomposition of N_{1S} XPS spectrum in Fig. 5b–d gives four peaks, i.e., pyridine nitrogen (pyridinic N, 398.4 eV), pyrrole type nitrogen (pyrrolic N, 400.0 eV), graphite type nitrogen (graphitic N, 401.0 eV) and oxidized nitrogen (oxidized N, 402.6 eV) [29]. As listed in Table 2, the contents of pyridinic N, pyrrolic N and oxidized N decrease except graphitic N in all samples. Obviously, heat treatment at comparable high temperature may enhance the production of graphitic N. However, pyridinic N, pyrrolic N and oxidized N have been decomposed as heat temperature increases.

Some literatures [30,19] have mentioned that when treated at 500 °C, catalyst forms 1 metal ion coordinated by 4 N atoms active sites, to form M–N_4–C. Therefore, more M–N_4–C will form with the increase of treated temperature. However, when heat temperature is ranged from 600 to 800 °C, M–N moiety may partially or completely decompose to form new catalytic sites. These sites consist of 1 metal coordinated by 2 N atoms to form M–N_2–C. M–N_4–C are the major active sites at low temperature (lower than 600 °C), while M–N_2–C moiety can form at temperature as high as 700 °C.

Table 2
The ratio analysis of the peaks in XPS spectra of the catalysts.

Sample	%C	%O	%Co	%Si	% N				
					Total	Pyridinic	Pyrrolic	Graphitic	Oxidized
Co–N–C-300/SiO_2	54.44	31.08	0.31	12.79	1.37	19.94	17.62	27.37	45.07
Co–N–C-500/SiO_2	57.15	28.84	0.36	12.53	1.12	14.04	16.30	46.97	22.69
Co–N–C-700/SiO_2	61.33	25.72	0.42	10.38	2.15	10.75	8.23	67.31	13.71

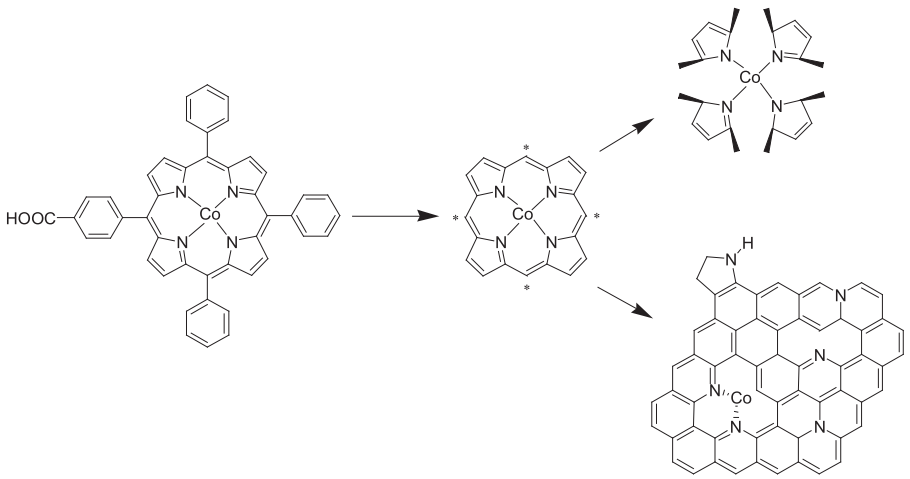

Fig. 6. The formation of Co–N–C with the heat treatment of CoTPP/SiO_2 in N_2 atmosphere.

Table 3
Catalytic performance of Co–N–C/SiO_2 for ethylbenzene oxidation[a]

Catalysis	Conversion (%)	Selectivity (%)[b]			Reusability (%)		
		AP	PA	BD	1st run	2nd run	3rd run
Co–N–C-300/SiO_2	13.6	64.6	32.2	3.2	13.5	8.1	6.0
Co–N–C-400/SiO_2	24.0	77.1	20.7	2.2	23.9	17.4	16.3
Co–N–C-500/SiO_2	30.4	74.2	23.1	2.7	30.3	23.6	16.0
Co–N–C-600/SiO_2	22.9	74.9	21.7	3.4	22.8	16.3	15.5
Co–N–C-700/SiO_2	22.3	78.8	17.7	3.5	22.2	16.7	13.2
Blank	4.3	59.0	34.5	6.5	–	–	–

[a] Reaction conditions: catalyst 30 mg, ethylbenzene 10 ml, O_2 pressure 8.0 atm, temperature 120 °C, and reaction time 5 h.
[b] Acetophenone (AP), Phenthyl Alcohol (PA), Benzaldehyde (BD).

Combined the fact mentioned in TG–DTA, the formation of Co–N–C with the heat treatment of CoTPP/SiO_2 in N_2 atmosphere has been presented in Fig. 6.

3.2. Activity measurement

Catalytic activity of catalysts for ethylbenzene oxidation is listed in Table 3. Obviously, the blank experiment (or called as autocatalysis system), compared to Co–N–C/SiO_2, shows relatively low catalytic activity for ethylbenzene oxidation. The ethylbenzene conversion is 4.3%. However, the activity of Co–N–C/SiO_2 with the heating temperature increasing in the range from 300 °C to 700 °C exhibits volcano-shape trend. And Co–N–C-500/SiO_2 presents the best catalytic activity for ethylbenzene oxidation, compared with other catalysts. Namely, the ethylbenzene conversion over Co–N–C-500/SiO_2 is 30.4%, much higher than that over Co–N–C-300/SiO_2, Co–N–C-400/SiO_2, Co–N–C-600/SiO_2 and Co–N–C-700/SiO_2, whose ethylbenzene conversions are 13.6%, 24.0%, 22.9% and 22.3%, respectively. Herein, combined the fact of XPS results, it is logical to deduce that M–N_4–C on catalysts is the most active sites for ethylbenzene oxidation.

In addition, the reusability of catalysts was also investigated. The catalyst was recovered by washing with ethanol and drying at 80 °C for 12 h and then reused to catalyze ethylbenzene oxidation. As shown in Table 3, all of catalysts exhibit comparably high activity for ethylbenzene oxidation at first run. Nevertheless, the activity of these catalysts suffers from a sharp decrease at second run. But this trend has been alleviated at third run. Taking Co–N–C-500/SiO_2 as example, the ethylbenzene conversion over Co–N–C-500/SiO_2 is as high as 30.3% at first run. However, the ethylbenzene conversion is sharply lowered to 23.6% at second and third run. As listed in Table 3, the catalysts heated at temperature lower than 600 °C may all suffer from this disability. This may be assigned to the easy decomposition of active sites such as Co–N_4–C at oxidation atmosphere. However, as for the catalysts treated at temperature higher than 600 °C, this disability has been alleviated. For example, the ethylbenzene conversion over Co–N–C-700/SiO_2 at first, second and third run is 22.2%, 16.7% and 13.2%, respectively. The ethylbenzene conversion seems similar if the loss of catalysts during the recovering process has been considered. Evidently, catalysts treated at high temperature will be beneficial to improve the reusability due to the thermal stability of Co–N_2–C.

4. Conclusions

Heat treatment plays a crucial role in the properties of Co–N–C/SiO_2 and their catalytic performance for ethylbenzene oxidation. It is shown that the ethylbenzene conversion over Co–N–C/SiO_2 heated at 500 °C is 30.3%, much higher than those over Co–N–C-300/SiO_2, Co–N–C-400/SiO_2, Co–N–C-600/SiO_2 and Co–N–C-700/SiO_2. In addition, Co–N–C/SiO_2, which can be effectively and effortlessly recovered, can retain high catalytic activity after reused for three times. Hereafter, it comes to the conclusion that Co–N–C species originated from heat treatment of C, N and metal ions in CoTPP/SiO_2 can effectively produce active catalytic sites and M–N_4–C is the most essential active sites for ethylbenzene oxidation.

Acknowledgements

The authors gratefully acknowledge the financial support from Natural Science Foundation of China (Nos. 21103045, 1210040, 1103312) and the Fundamental Research Funds for the Central Universities.

References

[1] S. Rochat, C. Minardi, J.Y. DeSaintLaumer, A.H. Herrmann, Chim. Acta 83 (2000) 1645.
[2] Z. Li, C.G. Xia, X.M. Zhang, J. Mol. Catal. A: Chem. 185 (2002) 47.
[3] T. Mallat, A. Baiker, Chem. Rev. 104 (2004) 3037.
[4] S.M. Ribeiro, A.C. Serra, A.M.d'A. Rocha Gonsalves, J. Mol. Catal. A: Chem. 326 (2010) 121.
[5] M. Halma, A. Bail, F. Wypych, S. Nakagaki, J. Mol. Catal. A: Chem. 243 (2006) 44.
[6] M. Mukherjee, A.R. Ray, J. Mol. Catal. A: Chem. 266 (2007) 207.
[7] D.H. Shen, L.T. Ji, Z.G. Liu, W.B. Sheng, C.C. Guo, J. Mol. Catal. A: Chem. 379 (2013) 15.
[8] H. Jahnke, M. Schonbron, G. Zimmerman, Top. Curr. Chem. 61 (1976) 133.
[9] H. Alt, H. Binder, G. Sandstede, J. Catal. 28 (1973) 8.
[10] R. Jiang, D. Chu, J. Electrochem. Soc. 147 (2000) 4605.
[11] P. Gouerec, A. Biloul, O. Contamin, G. Scarbeck, M. Savy, J. Riga, L.T. Weng, P. Bertand, J. Electroanal. Chem. 422 (1997) 61.
[12] G. Gruenig, K. Wiesener, A. Kaisheva, S. Gamburtsev, I. Iliev, Elektrokhimiya 19 (1983) 1571.
[13] L.H. Lu, R. Capek, A. Kornowski, N. Gaponik, A. Eychmuller, Angew. Chem. Int. Ed. 44 (2005) 5997.
[14] M. Humenik, W.D. Kingery, J. Am. Ceram. Soc. 37 (1954) 18.
[15] K.A.D.F. Castro, A. Bail, P.B. Groszewicz, G.S. Machado, W.H. Schreiner, F. Wypych, S. Nakagaki, Appl. Catal. A: Gen. 386 (2010) 51.
[16] H. Yoshino, K. Kamiya, H. Nasu, J. Non-Cryst. Solids 126 (1990) 68.
[17] G. Huang, T.M. Li, S.Y. Liu, Appl. Catal. A: Gen. 371 (2009) 161.
[18] A. Widelov, Electrochim. Acta 38 (1993) 2493.
[19] G. Faubert, G. Lalande, R. Cote, D. Guay, J.P. Dodelet, L.T. Weng, P. Bertrand, G. Denes, Electrochim. Acta 41 (1996) 1689.
[20] G.Q. Sun, J.T. Wang, R.F. Savinell, J. Appl. Electrochem. 28 (1998) 1087.
[21] S.Lj. Gojkovic, S. Grupta, R.F. Savinell, J. Electroanal. Chem. 462 (1999) 63.
[22] S.Lj. Gojkovic, S. Gupta, R.F. Savinell, Electrochim. Acta 45 (1999) 889.
[23] X. Guo, D.H. Shen, Y.Y. Li, M. Tian, Q. Liu, C.C. Guo, Z.G. Liu, J. Mol. Catal. A: Chem. 351 (2011) 174.
[24] G. Lalande, R. Cote, G. Ramizhmani, D. Guay, J.P. Dodelet, L. Dignard Bailey, L.T. Weng, P. Bertrand, Electrochim. Acta 40 (1995) 2635.
[25] K. Lee, L. Zhang, J. Zhang, J. Power Sources 170 (2007) 291.
[26] J. Maruyama, I. Abe, J. Electrochem. Soc. 154 (2007) 297.
[27] L.Z. Zheng, K. Tao, Y. Dan, K. Han, Y. Ji, Acta Chim. Sin. 70 (2012) 2342.
[28] K. Niu, B. Yang, J. Cui, J. Jin, X. Fu, Q. Zhao, J. Zhang, J. Power Sources 243 (2013) 65.
[29] Y. Okamoto, T. Imanaka, Appl. Catal. 73 (1991) 249.
[30] A.L. Bouwkamp-Wijnoltz, W. Visscher, J.A.R. van Veen, E. Boellaard, A.M. van der Kraan, S.C. Tang, J. Phys. Chem. B 106 (2002) 12993.